Available online at www.sciencedirect.com
SCIENCE DIRECT
Thermochimica Acta 441 (2006) 8–15
thermochimica acta
www.elsevier.com/locate/tca

Characterization of chromium-induced apoptosis in cultured mammalian cells: A differential scanning calorimetry study

Jamlet Monaselidze[a,*], Marina Abuladze[a], Nino Asatiani[a], Eugene Kiziria[a], Shota Barbakadze[a], George Majagaladze[a], Manana Iobadze[b], Leila Tabatadze[a], Hoi-Ying Holman[c], Nelly Sapojnikova[a,*]

[a] *Institute of Physics, Georgian Academy of Sciences, 6 Tamarashvili Str., 0177 Tbilisi, Georgia*
[b] *Institute of Medical Biotechnology, Georgian Academy of Sciences, 2 Chiaureli Str., 0159 Tbilisi, Georgia*
[c] *Center for Environmental Biotechnology, E.O. Lawrence Berkeley National Laboratory, 1 Cyclotron Road, Berkeley, CA 94720, USA*

Received 26 May 2005; received in revised form 3 November 2005; accepted 11 November 2005
Available online 20 December 2005

Abstract

The present study examined the cytotoxic effect of increasing Cr(VI) concentrations on cultured cells by a combination of biochemical methods and DSC, a novel use of DSC in the study of cell death. The characteristics of apoptotic cells are compared with normal cells. Chromatin in human epithelial-like L-41 cells has two thermal transitions at 100 and 105 °C. The heat from these endotherms is 90.5 ± 11.0 J/g DNA. The total heat of denaturation (Q_d) is 27.5 ± 3.5 J/g dry biomass. The heat evolved ($-Q$) is 15.6 ± 3.0 J/g dry biomass. The treatment of cells with 20 μM Cr(VI) for 2 and 4 h has not revealed any changes in heat of denaturation and heat evolution ($-Q$). However increased treatment time with Cr(VI) at 20 μM resulted in significant changes to the thermal profile and a sharp linear decrease of ($-Q$) and Q_d values. The Q_d and ($-Q$) values of cells treated with 20 μM Cr(VI) for 48 h are equal to 15.5 ± 2.0 and 2.1 ± 0.4 J/g dry biomass, respectively. The changes in chromatin conformation, Bax expression and the collapse of the mitochondrial membrane permeability coincide with the time point from which the action of chromium is irreversible.

Keywords: Calorimetry; Hexavalent chromium (Cr(VI)); Bax expression; Mitochondrial membrane permeability

1. Introduction

Chronic chromium exposure can have serious pathological consequences. Results from decades of human and animal model studies indicate that at high concentrations Cr(VI) poses serious health hazards in terms of both its potential toxicity and carcinogenicity [1–5]. Soluble and insoluble hexavalent chromium salts have been demonstrated to induce morphological and neoplastic transformation and mutagenicity in human cells [6]. The potential carcinogenic activity was less frequently evident with Cr(VI) compounds having a low solubility [7]. In the cellular environment, Cr(VI) exists as a chromate oxyanion $[CrO_4]^{2-}$, which penetrates the cell through the sulfate and phosphate ion transporters [1]. Cr(VI) directly generates reactive oxygen species (ROS) by interaction with cellular reductants. During the reduction of Cr(VI), a whole spectra of ROS are produced [8]. ROS can cause lipid peroxidation and oxidation of some enzymes and a massive protein oxidation and degradation [9]. Reactive oxygen species are considered as one of the possible signals to initiate and/or maintain cell apoptosis [10].

During Cr(VI) intracellular reduction a wide variety of DNA lesions, such as Cr-DNA adducts [11,12], DNA strand breaks [13], DNA–DNA crosslinks [4,14] and DNA–protein crosslinks [15,16] are generated. These could be the products of ROS accompanying intracellular Cr(VI) reduction to Cr(V), Cr(IV) and Cr(III) species and/or the direct binding of Cr(V)-complexes

* Corresponding authors. Tel.: +995 32 396716; fax: +995 32 391494.
E-mail addresses: jamlet_monaselidze@yahoo.com (J. Monaselidze), nellys@iphac.ge (N. Sapojnikova).

0040-6031/$ – see front matter © 2005 Elsevier B.V. All rights reserved.
doi:10.1016/j.tca.2005.11.025

and Cr(III) to DNA. Genotoxic damages are one of the possible apoptosis determinants of a chromium-exposed cell [17].

Single strand breaks in DNA under chromium action occurred rapidly and were easily repaired, while DNA–protein crosslinks developed slowly and were not easily repaired as the dose was progressively increased to substantially toxic levels of Cr(VI) [4,18]. These data have been obtained mainly for high concentrations of Cr(VI) and short times of treatment. However, for some established cell lines, low to moderate and serious levels of DNA damages were observed under low doses of Cr(VI) [19,20].

In our previous study [21] it was shown that Cr(VI)-treated human epithelial-like L-41 cells died by apoptosis, as identified by morphological analysis, the activation of caspase-3 and DNA fragmentation. The toxic activity of chromium (20 μM) inhibits cellular antioxidant defenses and enhances intracellular oxidized state, which results in inducing and/or maintaining the death programs in cells. Our data are consistent with published observations regarding the involvement of oxidative stress and cell death via apoptosis in the toxicity of Cr(VI) [8,19]. Cells treated with Cr(VI) exhibit apoptotic features, depending on cell line, dose and exposure time; 300 μM Cr(VI) after 3 h of exposure causes apoptosis in 24 h in human lung tumor A549 cells [8], a 24 h exposure to 12.5 μM Cr(VI) is apoptogenic for chronic myelogenous leukemic K562 cells, for cultured J774A.1 murine macrophage cells, 0.6 μM Cr(VI) is toxic after 48 h [19].

The purpose of the present study is to establish the temporal consequence of low doses of Cr(VI) on the stability of subcellular structures, particularly on the structure of chromatin in situ by differential scanning calorimetry (DSC).

Investigation of chromatin structure in whole nuclei, cells, and tissues by DSC has been carried out for the last two decades [22,23]. DSC enabled changes in chromatin structure in whole cells caused by various external agents to be investigated. It was demonstrated that low concentrations of *cis*-$[Pt(GuO)_2(GuOH)_2]$ administrated to Balb/c mice formed crosslinks in liver DNP (desoxiribonucleoprotein) complex, leading to increased chromatin thermostability and high concentrations caused DNA damage resulting in decreased thermostability [24]. DSC study of dilute solutions of DNA, isolated from various organs of C3HA and Balb/c mice exposed to low concentrations of $NiCl_2$ and $NiSO_4$ (intraperitoneally), showed severe damage in DNA structure [22]. Our results demonstrate that treatment of L-41 cells for 24 h with 20 μM Cr(VI) causes damage to cytoplasmic structures and dysfunction of mitochondria along with lesions of nuclear DNA.

2. Materials and methods

2.1. Cell culture

The L-41 cell line is an established human epithelial-like cell culture (Research Center of Medical Genetics, Russian Academy of Medical Science, Moscow, Russia) that was derived from J-96 cell line originally obtained from a patient with monocytic cell leukemia [25]. The L-41 cell line was secondary routinely established and subcloned by viral transformation (Coxsackie B-3), and was characterized by high proliferative capacity and adherent cell growth as epithelial-like monolayer culture with human karyotype [26]. Flow cytometry analysis showed that the polyploid cell fractions never exceed 3% in control cultures (data not shown). The L-41 cells were maintained as adherent cells in Eagle's culture medium supplemented with 10% donor calf serum, 2 mM L-glutamine, 100 units of penicillin/ml, and 100 μg of streptomycin/ml at 37 °C in a 5% CO_2 incubator. Cells were harvested with trypsin (0.25%)/Na_2EDTA solution.

2.2. Chromium treatment and viability assay

L-41 cells were seeded at 3×10^4 cells per well in 200 μl culture medium in 96-well microtiter plates and cultured to 80% of confluence for 48 h. Cr(VI) at 1, 2, 5, 10, 20 and 30 μM was added as potassium chromate and the cells continued to grow for 2, 4, 17, 24 and 48 h. Viability of chromium-exposed L-41 cells was assessed by the ability of viable cells to convert the tetrazolium dye MTT (3-[4,5-dimethylthiazol-2-yl]-2,5-diphenyltetrazoliumbromide) to a water-insoluble formazan dye, which is based on the activation of succinate dehydrogenase [27,28]. The culture medium was removed and the colored precipitate was solubilized with dimethyl sulfoxide (DMSO). After 30 min, cell survival and background was determined by absorbence at 570 and 660 nm, respectively. The percentage of viable cells was calculated with reference to control cells. In these assays, four wells were usually examined for each concentration and time point. The data are the result of three independent experiments.

2.3. Detection of apoptosis: assessment by morphological analysis, Bax expression, mitochondrial membrane potential stability

Cell population was analyzed by fluorescent microscopy after staining with acridine orange (AO) for the detection of apoptotic cells [29]. Cells were grown on the cover slides before the analysis and examined with an ×40 dry objective. Apoptotic nuclei can be detected by highly condensed chromatin.

A Western blot assay was performed using antibodies against Bax and secondary anti-rabbit IgG (Sigma, USA). The reaction took place with ECF substrate (Santa-Cruz, USA). The cell pellet was treated with lysis buffer M-PER® Mammalian Protein Extraction Reagent (Pierce, USA) following the manufacturer instructions. Sodium dodecyl sulfate polyacrylamide gel electrophoresis (SDS-PAGE) was performed by using 15% gel [30]. Fifty micrograms of total protein was run per lane. The resolved proteins were transferred to a nitrocellulose membrane. Actin (Sigma, USA) expression served as an internal control for protein loading.

Mitochondrial membrane potential in situ is an important indicator of mitochondrial function and dysfunction. A flow cytometry method was used for quantitative measurement of mitochondrial membrane potential with the lipophilic, cationic fluorescent probe 3,3-dihexyloxacarbocyanine iodide—$DiOC_6$ [31]. Twenty microliter of 0.2 μM solution of $DiOC_6$ was added

per 10^5 cells for 15 min at 37 °C and analyzed by flow cytometry using FACScan instrument (Becton Dickinson). Excitation of $DiOC_6$ was at 488 nm; emission was measured at 530 nm.

2.4. DSC

DSC was carried out with a modified DSC originally designed at the Institute of Physics of the Georgian Academy of Sciences [32,33].

The detection limit of the DSC is 0.1 μW, temperature range is 5–150 °C and the measuring capsule volume is 0.3 cm^3. The calorimeter resolution of heat capacity (i.e. significant deviation from the baseline) is 10 μJ/°C. The accuracy of absolute temperature measurement is better than 0.05 °C. Measurements were carried out at 1 point per 1 s at scan rates from 0.04 to 1 °C/min. The calculation of metabolic heat ($-Q$), heat of denaturation (Q_d), denaturation temperature (T_d) and width of the peak at half height (ΔT_d) was carried out by a program developed by us. Deconvolution of curves was conducted with Origin 6.0 (Microcal™ Software Inc.). At scan rates from 0.04 to 0.25 °C/min, the means of T_d, ΔT_d and Q_d of the endotherms were unchanged. The process of subcellular structure denaturation is thus close to equilibrium under these conditions. The error in determination $-Q$ and Q_d of L-41 cells was less than 12%. T_d was determined to ±1 °C and ΔT_d to ∼0.5 °C.

For DSC, L-41 cells were cultured to 80% of confluence for 48 h in flasks with the seeding concentration 3×10^5/ml. Cr(VI) at 2, 5, 10 and 20 μM was added as potassium chromate and the cells continued to grow under Cr(VI) action for 2, 4, 17, 24 and 48 h. The cells were harvested by centrifugation at 1000 × g for 10 min. The pellet was resuspended in culture medium and transferred into the DSC capsule. There was culture medium in the reference capsule to compensate for the contribution of heat absorption/evolution by serum structures. The determination of dry weight of cell biomass was performed as in [23]. The mean DNA content in an L-41 cell was taken as in a human diploid cell, 6.9×10^{-12} g of DNA per cell.

3. Results

3.1. Dose effect of Cr(VI) on cell viability

The results of Cr(VI) action on cell viability in the concentration range of 1–30 μM after 24 and 48 h of permanent exposure without medium replenishment are presented in Fig. 1. Chromium caused dose-dependent loss of viability.

One to 5 μM chromium did not induce the cytotoxic effect in the L-41 cell culture. A high percentage of cell viability was detected up to 96 h of exposure to these concentrations of chromium (data not shown). Ten μM Cr(VI) decreased cell viability to 65% after 24 and 48 h. Exposure to 20 μM Cr(VI) caused toxic effect at 24 h (50% of viable cells) and only 15% at 48 h.

In our previous study, the time-dependent loss of cell viability at 20 μM Cr(VI) was accompanied by the increased level of apoptotic cells [21]. Morphological analysis using fluorescent microscopy shows that chromatin condenses and aggregates into dense compact masses under 20 μM Cr(VI) for 48 h (Fig. 2). These changes are consistent with apoptosis. The results show 20 μM Cr(VI) as the toxic apoptogenic concentration, which was used for the experimental system.

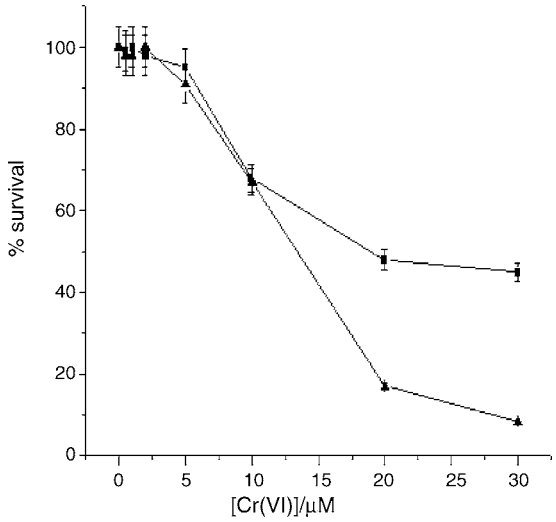

Fig. 1. Effect of Cr(VI) on L-41 cell viability. Exponentially growing cells were treated with the indicated concentration of Cr(VI) for 24 h (■) and for 48 h (▲). Cell survival was assessed by MTT assay.

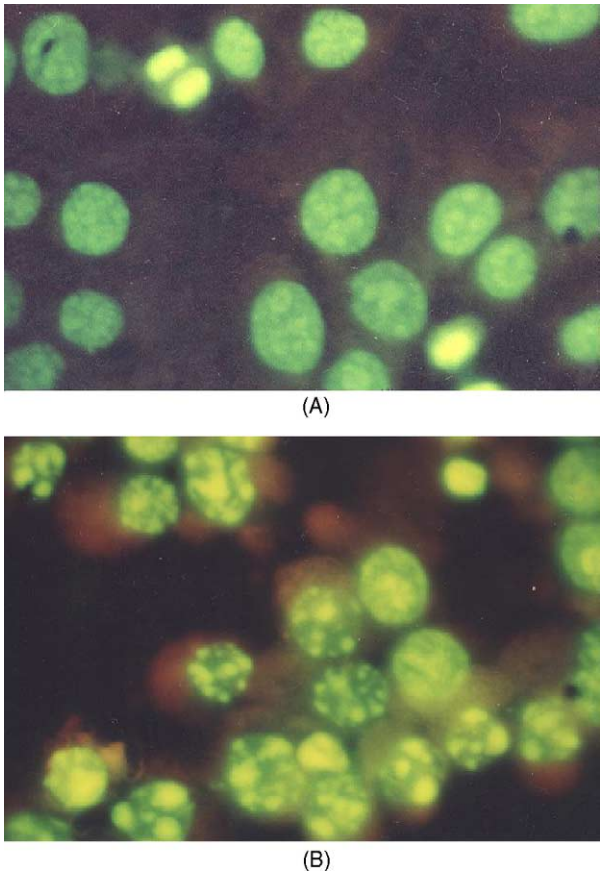

Fig. 2. L-41 cell morphology examined under a fluorescent microscope after staining with Acridin Orange (×400): (A) cells without chromium action, 96 h of growth; (B) cells under 20 μM Cr(VI) action for 48 h (80–90% of apoptotic cells in the population).

3.2. Expression of Bax and instability of mitochondrial membrane under toxic Cr(VI) action

To check that chromium-induced apoptosis in L-41 cells involves over-expression of Bax, a protein promoting apoptosis, the level of this protein under toxic chromium concentrations was estimated by Western blot analysis. The expression of Bax in L-41 cells before and after various times of Cr(VI)-treatment are presented in Fig. 3A. The results indicate an increase in Bax protein after 17 h of 20 μM Cr(VI) treatment.

Bax translocates to the mitochondria and induces cell death by mitochondrial dysfunction, by favoring the instability of mitochondrial membrane [34]. Mitochondrial function is monitored by measuring the accumulation of cationic fluorescent probes in response to the mitochondrial transmembrane potential in viable cells. Loss of membrane potential is detected as a reduced $DiOC_6$ signal. The mitochondrial membrane potential was estimated through time points of the chromium action, at which no effect and high expression of Bax was observed, respectively (2 and 24 h) and at 48 h when the cell population represented 80–90% of apoptotic cells. Fig. 3B presents the flow cytometry data of $DiOC_6$ assay using L-41 cells under toxic chromium action. It has been shown that 20 μM Cr(VI) for 2 h caused little or no changes to mitochondrial permeability. However after 24 h significant lowering of mitochondrial potential was detected. The loss of mitochondrial membrane potential as one of the key events occurring in apoptosis was observed in Cr(VI)-exposed population of human fibroblasts [20] and human lung tumor A549 cells [8].

3.3. DSC of L-41 cells under standard cultivation conditions

The L-41 cell denaturation process from 10–120 °C is presented in Fig. 4A. An intense asymmetric peak of heat evolution with maximum at about 36.5 °C and with weakly expressed shoulder at about 20 °C due to metabolism and oxidation reactions is observed in the temperature range 10–40 °C with 12.1 ± 1.4 J/g dry biomass (Fig. 4A, curve 1). Three endotherms with three clear shoulders are observed in the temperature range 40–120 °C. Calculated integral heat of denaturation from the area under the endotherms and a baseline in the range 40–120 °C is 24.1 ± 2.3 J/g of dry biomass (Fig. 4A, curve 1). The endothermic processes are associated with melting of subcellular

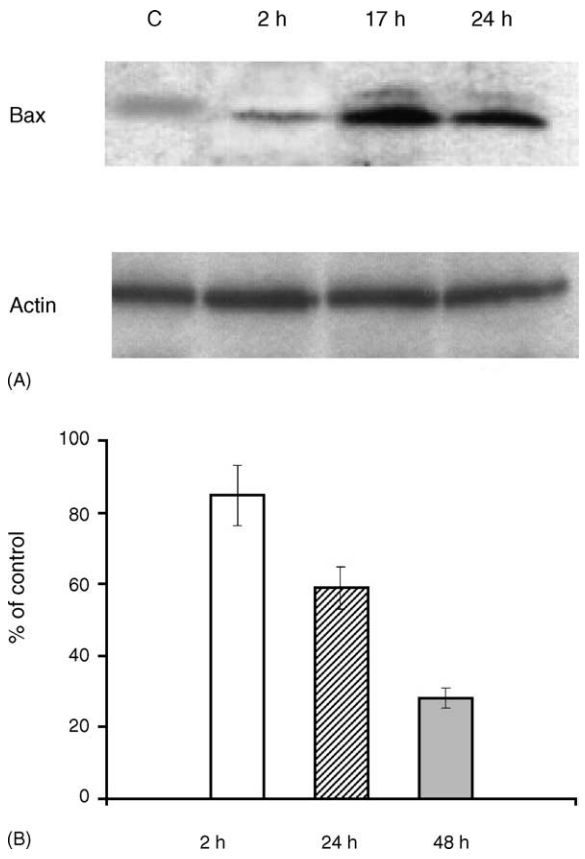

Fig. 3. (A) Expression of Bax protein in L-41 cells after 20 μM of Cr (VI) treatment. Immunoblots were probed with anti Bax antibody (Sigma) and developed by using chemilumeniscent detection kit (Santa-Cruz). Actin (Sigma, USA) expression served as an internal control for protein loading. (B) Mitochondrial membrane potential of L-41 cells in response to 20 μM Cr(VI) action measured by carbocyanine dye $DiOC_6$ signal intensity and expressed as a percentage of the control.

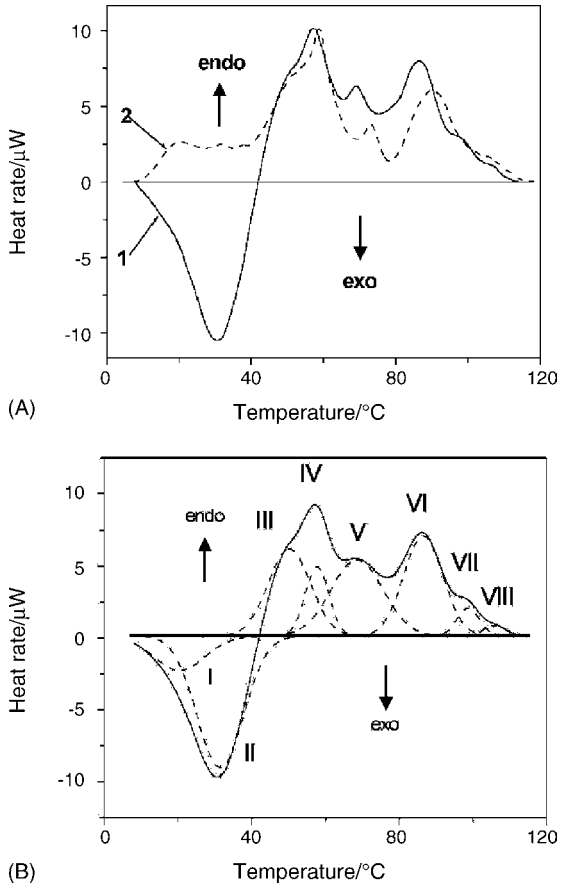

Fig. 4. (A) Thermal effects observed during heating of L-41 cells in culture medium (pH 7.2). Curve 1 (solid line), ~2×10^7 cells (dry biomass is 6.9 mg; DNA is 0.11 mg); heating rate 0.1 °C/min. Curve 2 (dash line), cells heated to 41 °C and cooled for 30 min to 5 °C and again heated with heating rate 0.76 °C/min (dry mass is 6.5 mg; DNA is 0.10 mg). The endotherms shift to higher temperature in curve 2 is caused by the scan rate increase. (B) Deconvolution of curve 1.

structures. Proteins, nuclear matrix, ribosome complex and other structure components in cytoplasm denature in the temperature range 42–85 °C; chromatin denatures in the temperature range 75–120 °C [23,35–40].

When L-41 cell suspension was heated to 41 °C and then cooled for 30 min to 5 °C, the curve was significantly changed. As shown in Fig. 4A, curve 2, no heat was evolved in the temperature range 10–40 °C. Instead, the endotherms appeared as weak peaks at 20 and 37 °C. The heat of denaturation, $Q_d = 3.5 \pm 0.3$ J/g dry biomass. The endotherms in the range 40–120 °C are shifted 1–2 °C lower (at heating rate from 1.0 to 0.12 °C/min), without changing the total heat, and are not changed at heating rate lower than 0.12 °C/min. Thus, the integral heat ($-Q$) evolved in the temperature range 10–40 °C is equal to 15.6 ± 3.0 J/g dry biomass. The value of heat evolution ($-Q$) is in good agreement with the heat production of T-lymphoma cells determined by isothermal calorimetry in anaerobic conditions [41]. The preliminary heating of L-41 cells to 41 °C and subsequent cooling was carried out for exact determination of total ($-Q$) value through the inhibition of cell respiration. The data presented in Fig. 4A show that the disappearance of the exotherm is not connected with denaturation of subcellular structures, because the profile of the endotherms has not changed significantly. We propose that cell respiration contribute significantly to ($-Q$). A similar result was observed for Spirulina *platensis* cells [23,40].

The total heat of denaturation, calculated from areas under the peaks of the endotherms in the temperature range 40–120 °C (Fig. 4A, curve 2), is equal to 27.5 ± 3.5 J/g dry biomass and coincides with Q_d value determined for rat hepatocytes [42,43].

The deconvolution of the heat flow rate curve (Fig. 4A, curve 1) on elementary Gaussian constituents was carried out and presented in Fig. 4B. A similar approach has been used previously [23,36,42]. The deconvolution reveals eight thermal transitions in the temperature range 10–120 °C. The temperature range from 40 to 120 °C was resolved into six endotherms (III–VIII) with the respective T_d at 50, 59, 74, 88, 100 and 105 °C.

DSC affords a measure of the degree of chromatin condensation in situ. Chromatin in nuclei isolated from rat hepatocyte persistent nodules has two thermal transitions at 75 and 90 °C and in the case of nuclei from early developing nodules—three thermal transitions at 75, 90 and 107 °C [36]. Calculation of nuclear chromatin heat of denaturation corresponding to the endotherms with $T_d = 75$, 90 and 107 °C gave $Q_d = 75.6 \pm 13.5$ J/g DNA. It is believed that the endotherm with $T_d = 107$ °C corresponds to the denaturation of the core particle packaged within the 30 nm-thick fibers. The endotherm with $T_d = 90$ °C corresponds to DNA melting of tightly packed nucleosome in 10 nm filaments which result from the decondensation of 30 nm-thick fibers. The endotherm with $T_d = 75$ °C corresponds to melting of internucleosomal DNA weakly defended by HI histone [36,42].

To find out which endotherms in the temperature range 75–120 °C correspond to the denaturation of chromatin DNA in the case of L-41 cells, the total heat of chromatin denaturation from the endotherms VI, VII, VIII was estimated. Q_d is 289.2 ± 30 J/g DNA, taking into account the number of cells in suspension, mass in the measuring capsule of calorimeter, and the mean DNA content. The obtained value is significantly higher than Q_d (ΔH_d) of nuclear chromatin of eukaryotes. But if the calculation of Q_d was performed on the basis of the endotherms VII, VIII, a value equal to 90.5 ± 11 J/g DNA was obtained, which coincides with the value of $Q_d = 75.6 \pm 13.5$ J/g DNA [36,43]. Thus, we come to the conclusion that chromatin in the composition of L-41 cells has two thermal transitions at 100 °C and 105 °C, and the heat of chromatin denaturation in both thermal transitions is $Q_d = 90.5 \pm 11$ J/g DNA. Each transition corresponds to a structurally distinguishable domain of chromatin DNA.

Considering the data presented in [32,44,45], and the fact that DNA denaturation enthalpy ΔH_d (Q_d) depends linearly on denaturation temperature, we have calculated that the DNA melts in chromatin with $Q_d = 58.5 \pm 4.1$ J/g. The remaining 31.8 J/g relates to the denaturation of proteins responsible for organization of high order chromatin structure in vivo. According to [46,47], ΔH_d of small globular proteins at 100–105 °C is equal to 55.4 J/g and for H1 histone, 32.8 J/g. As the ratio DNA/protein is equal to ~1.0 in chromatin, the value 31.8 J/g is a realistic value for denaturation enthalpy of chromatin proteins.

The heat absorption for chromatin denaturation was calculated from the area under the endotherms VII and VIII and was equal to 1.76 ± 0.25 J/g dry biomass. It makes up 6.4 % of total Q_d (27.5 ± 0.3 J/g dry biomass) and does not contribute significantly to total Q_d. Therefore, the main contribution in the total heat of denaturation comes from the melting of proteins, membranes and other structure components in a cell.

3.4. Characteristics of L-41 cells under Cr(VI) action

The percentage of L-41 cells keeping their vital functions after treatment with potassium chromate was calculated on the basis of calorimetric data. The ($-Q$) value, calculated for untreated L-41 cells, equals 15.6 J/g dry mass and corresponds to 100% survival. From the ($-Q$) values for L-41 cells treated with 10 and 20 μM Cr(VI) for 48 h (8.5 and 2.1 J/g dry biomass, respectively), the percent of cell survival was 54 and 13%, respectively (Fig. 5A and B). MTT cytotoxicity assay shows that 2 μM Cr(VI) did not induce the cytotoxicity at 48 h, whereas 10 μM Cr(VI) decreased cell viability to 65%. Treatment with 20 μM Cr(VI) decreased viable cell population to 15% after 48 h. Comparison of the dependence of heat evolved on Cr(VI) concentration with cell viability under Cr(VI) agrees with cell viability estimated by MTT assay. The plot of ($-Q$) values against the percent of cell viability estimated by MTT represents a regression line with a coefficient of correlation of 0.983.

The dependence of Q_d on the concentration of Cr(VI) treatment for 48 h shows the same character as the dependence of ($-Q$) on Cr(VI) dose (Fig. 5A). This means that subcellular structure damage (Q_d) and the decrease of vital functions ($-Q$) occur simultaneously and in a dose-dependent manner.

A similar picture was observed when the treatment time with 20 μM Cr(VI) was increased. Fig. 6 represents the dependence of heat evolved ($-Q$) and total heat of denaturation on time of 20 μM Cr(VI) exposure. ($-Q$) and Q_d values are not changed by

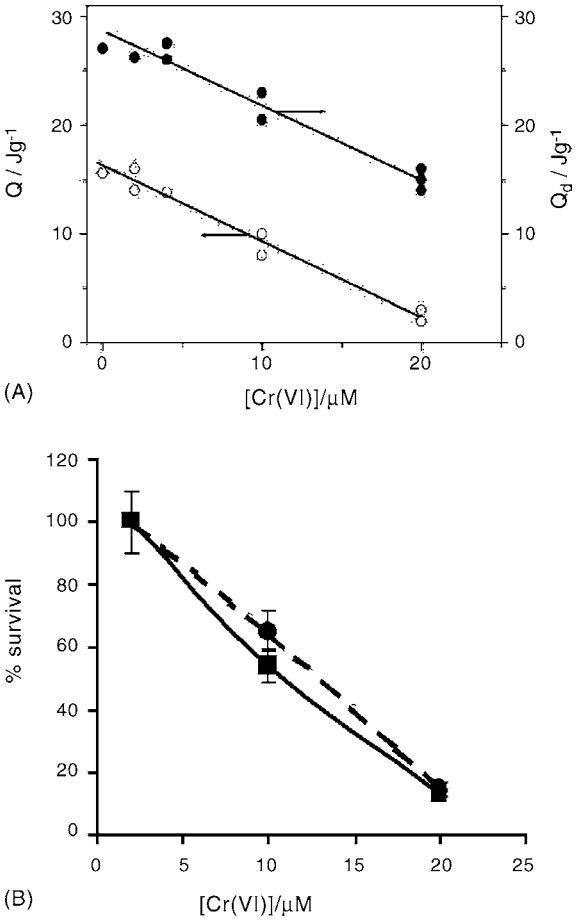

Fig. 5. (A) Heat evolved ($-Q$) (◯) and total heat of denaturation Q_d (●) after treatment of L-41 cells with various concentrations of Cr(VI) for 48 h. Conditions as in Fig. 4. (B) Survival of L-41cells after 48 h of chromium action estimated by DSC (■) and MTT (●) methods.

20 μM Cr(VI) for 2 and 4 h, but as the treatment time increases, the values of ($-Q$) and Q_d decrease.

The thermal profile of L-41 cells treated with 20 μM Cr(VI) for 24 and 48 h are presented in Fig. 7. The increased incubation time caused a decrease of ($-Q$) and Q_d values (Fig. 6), and also a significant change in the thermal profile of L-41 cells. After

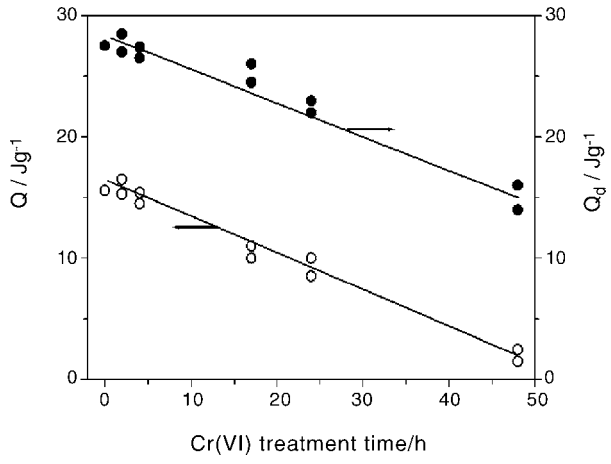

Fig. 6. The time-dependent effect of 20 μM Cr(VI) on heat evolved ($-Q$) (◯) and total heat of denaturation Q_d (●) of L-41 cells. Conditions as in Fig. 4.

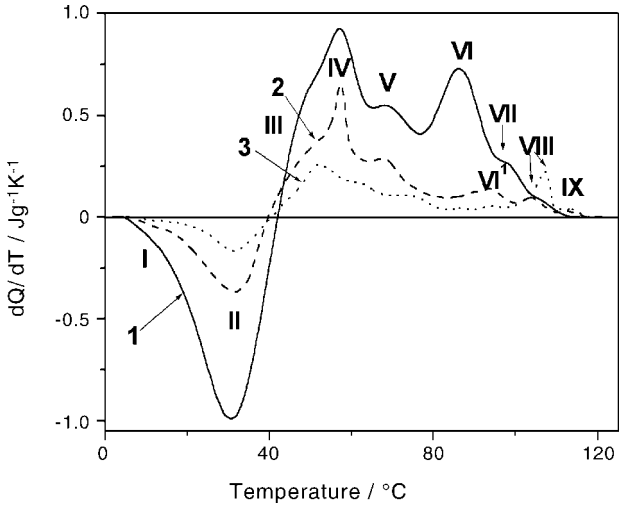

Fig. 7. dQ/dT of L-41 cells untreated (solid curve 1), treated with 20 μM Cr(VI) for 24 h (dash curve 2) and 48 h (dot curve 3). Conditions as in Fig. 4.

24 h of Cr(VI) action, endotherms VI and VII fully disappear, and new endotherms VI′ and IX at 93 and 112 °C appear (Fig. 7, curve 2). $Q_{d\ DNA}$ of the endotherms at 93, 105 and 112 °C are equal to 43.9, 27.1 and 8.7 J/g DNA, respectively.

The L-41 cells lost their adhesion to the culture plates after 48 h exposure to Cr(VI) to give the detached apoptotic cells (80–90% of the whole population) [21]. The thermal profile of apoptotic cells is presented in Fig. 7, curve 3. The size of endotherms IV, V and VI′ at 59, 71 and 93 °C is sharply decreased, and the endotherm at 107.5 °C is significantly increased and dominates the thermal curve. The intensity of the endotherm at 112 °C is not changed. Q_d calculated from endotherm areas with T_d at 93, 107.5 and 112 °C is decreased in comparison with 24 h of 20 μM Cr(VI) action only by 4.8 J/g DNA.

4. Discussion

The aim of the present study is to establish the sequence of Cr(VI) effects on the stability of subcellular structures, chromatin in situ and the development of apoptosis. The total heat of denaturation reflects the subcellular structure stability. The heat evolution ($-Q$) reflects cell survival. Both of these parameters decrease with time of exposure to 20 μM Cr(VI) (Figs. 6 and 7). The decrease of Q_d is connected with damage to membrane structures, proteins and subcellular structures as shown by the sharp decrease of endotherm intensity at 59 °C and disappearance of endotherms at 74 and 88 °C compared with endotherms IV, V, VI of the control curve (Fig. 7, curve 1). Proteins, nuclear matrix, ribosome complex and other components in cytoplasm denature in the temperature range 42–85 °C. Specific caspase-mediated cleavages of substructures, e.g., cleavage of the nuclear membranes, lamins, cytoskeletal proteins are mentioned in [48,49]. Cr(VI) induces apoptosis with the implication of caspase-3 pathway [21]. Thus, the dramatic changes in L-41 cells after the irreversible toxic time point could be the result of a indirect chromium-induced damage to subcellular structures,

namely membranes and proteins, as well as the result of caspase activation during chromium-induced apoptosis.

Disturbance of cell respiration accompanies the process of apoptosis [50]. Indeed, a sharp decrease of ($-Q$) after 24 h of 20 μM Cr (VI) exposure points to this. The exotherm ($-Q$) fully disappeared after preheating a suspension of L-41 cells at 41 °C. Recent studies suggest that mitochondria can be considered as the control center of cell death. The mitochondrial membrane potential, in situ, is a sensitive indicator of the physiological state of the mitochondria and the cell [51]. Distortion of mitochondrial membrane potential takes place at 24 h of Cr(VI) action, when the cell population shows the cells irreversibly undergoing apoptosis. Recent analysis has revealed that the outer mitochondrial membrane ruptures, at least during apoptosis induced by overexpression of the proapoptotic protein Bax [52]. Moreover, *Bax*, *Bak* doubly deficient cells are resistant to all intrinsic death signals tested, indicating that "multidomain" proapoptotic molecules are an obligate gateway to mitochondrial dysfunction and cell death [53]. Up-regulation of Bax was observed in L-41 cells from the time point when 20 μM Cr(VI) retains cytotoxicity.

DNA strands break and DNA–DNA, DNA–protein crosslinks increase under Cr(VI) in a dose-dependent manner and correlate with the decrease of cell survival [8,13–15]. The influence of toxic chromium concentration on the L-41 cell chromatin structure in situ was revealed only after 24 h in our study. The destabilization of chromatin structural domains melting at 100 °C has been observed after 24 h of 20 μM Cr(VI) action. The disappearance of endotherm VII (T_d = 100 °C) and the appearance of endotherm (VI′) at T_d = 93 °C with Q_d = 43.9 J/g DNA (Fig. 7, curve 2) points to this. Toxic chromium for 24 h may lead to the accumulation of DNA strand breaks, which leads to diminished thermostability of chromatin. Alternatively, destabilizing structural effects of chromium may be the result of DNA conformation modifications. High mobility group proteins 1 and 2 (HMGB1 and HMGB2) recognize chromium damaged DNA recovered from Cr(VI)-treated cells [54]. DNA binding by HMG-1/2 is DNA conformation dependent [55]. A characteristic feature of HMG proteins is their ability to recognize bent and unwound DNA structures like four-way junctions, cruciform DNA and *cis*-platin modified DNA [56,57].

The appearance of the weak new endotherm IX at 112 °C after 24 h of 20 μM Cr(VI) action could be attributed to the formation of chromium-mediated DNA–DNA and/or DNA–protein crosslinks, stabilizing a small part of chromatin structure. Two possible chemical classes of Cr–DNA interstrand complexes are observed in cell free systems, one that is stable to alkali but sensitive to heat, and a smaller class (about 10%) which is heat-stable [17].

The thermal profile of the detached apoptotic cells at 48 h of 20 μM Cr(VI) action reveals (Fig. 7, curve 3) that a sharp increase of Q_d of the endotherm at 107.5 °C due to 80% decrease of Q_d of the endotherm at 93 °C has been observed. The increase of T_d endotherm at 93 °C by 14.5 °C and narrowing of the corresponding ΔT_d by 5 °C could be explained by formation of a chromatin super-condensed state typical of apoptotic cells. Analysis of Cr(VI)-treated L-41 cells by fluorescence microscopy confirms changes in DNA compaction characteristic of apoptosis (Fig. 2B).

In summary, DSC curves of L-41 cells has revealed that 20 μM Cr(VI) after 24 h of incubation results in the formation of DNA lesions and damage to subcellular structures. The high level of DNA lesions, Bax expression and the decrease of the mitochondrial membrane permeability coincide with the time point from which the action of chromium is irreversible. The DSC method reflects the whole spectrum of the intracellular changes induced by toxic chromium concentrations and corroborates morphological and biochemical methods for estimation of apoptotic process.

Acknowledgment

This work was supported by G-349 Grant awarded by the International Science and Technology Center (ISTC).

References

[1] D. Stearns, K.E. Wetterhahn, in: N. Hadjiliadis (Ed.), Cytotoxic, Mutagenic and Carcinogenic Potential of Heavy Metals Including Metals Related to Human Environment, Kluwer Academic, Dordrecht, 1997, pp. 107–121.
[2] K. Liu, J. Husler, J. Ye, S.S. Leonard, D. Cutler, F. Chen, S. Wang, Zh. Zhang, M. Ding, L. Wang, X. Shi, Mol. Cell. Biochem. 222 (2001) 221–229.
[3] M. Costa, Tox. Appl. Pharmacol. 188 (2003) 1–5.
[4] T.J. O'Brien, S. Ceryak, S.R. Patierno, Mutat. Res. 533 (2003) 3–36.
[5] M. Valko, H. Morris, M.T.D. Cronin, Curr. Med. Chem. 12 (2005) 1161–1208.
[6] D. Bagchi, S.J. Stohs, B.W. Downs, M. Bagchi, H.G. Preuss, Toxicology 180 (2002) 5–22.
[7] S. De Flora, Carcinogenesis 21 (2000) 533–541.
[8] J. Ye, S. Wang, S.S. Leonard, Yi. Sun, L. Butterworth, J. Antonini, M. Ding, Yo. Rojanasakul, V. Vallyathan, V. Castranova, X. Shi, J. Biol. Chem. 274 (1999) 34974–34980.
[9] J.M. Mates, C. Perez-Gomez, I. Nunez de Castro, Clin. Biochem. 32 (1999) 595–603.
[10] G.K. Harris, X. Shi, Mutat. Res. 533 (2003) 183–200.
[11] V. Voitku, A. Zhitkovich, M. Costa, Nucleic Acids Res. 26 (1998) 2024–2030.
[12] T.J. O'Brien, H.G. Mandel, D.E. Pritchard, S.R. Patierno, Biochemistry 41 (2002) 12529–12537.
[13] J.W. Hamilton, K.E. Wetterhahn, Carcinogenesis 7 (1986) 2085–2088.
[14] J. Xu, G.J. Bubley, B. Detrick, L.J. Blankenship, S.R. Patierno, Carcinogenesis 15 (1996) 1511–1517.
[15] M. Sugiyama, S.R. Patierno, O. Cantoni, M. Costa, Mol. Pharmacol. 29 (1986) 606–613.
[16] R. Codd, C. Dillon, A. Levina, P. Lay, Coordin. Chem. Rev. 216–217 (2001) 537–582.
[17] J. Singh, D.L. Carlisle, D.E. Pritchard, S.R. Patierno, Oncol. Rep. 5 (1998) 1307–1318.
[18] M. Sugiyama, X.W. Wang, M. Costa, Cancer Res. 46 (1986) 4547–4551.
[19] D. Bagchi, M. Bagchi, S.J. Stohs, Mol. Cell. Biochem. 222 (2001) 149–158.
[20] D.E. Pritchard, S. Ceryak, L. Ha, J.L. Fornsaglio, S.K. Hartman, T.J. O'Brien, S.R. Patierno, Cell Growth Differ. 12 (2001) 487–496.
[21] N. Asatiani, N. Sapojnikova, M. Abuladze, T. Kartvelishvili, N. Kulikova, Eu. Kiziria, E. Namchevadze, H.-Y. Holman, J. Inorg. Biochem. 98 (2004) 490–496.
[22] E. Andronikashvili, V. Bregadze, J. Monaselidze, in: H. Sigel (Ed.), Metal Ions in Biological Systems, vol. 23, Marcel Dekker, New York, 1988, pp. 331–356.

[23] L. Topchishvili, Sh. Barbakadze, A. Khizanishvili, G. Majagaladze, J. Monaselidze, Biomacromolecules 3 (2002) 415–420.
[24] J. Monaselidze, Ja. Kalandadze, Z. Chanchalashvili, G. Majagaladze, Biophysics 37 (1992) 36–39.
[25] E.E. Osgood, J.H. Brooke, Blood 10 (1955) 1010–1022.
[26] V.D. Solov'ev, N.E. Gulevich, Acta Virologica 4 (1960) 220–226 (in Russian).
[27] J. Carmichael, W. DeGraff, A. Gardar, J. Minna, J. Mitchell, Cancer Res. 47 (1987) 936–942.
[28] D. Bagchi, M.X. Tran, S. Newton, M. Bagchi, S.D. Ray, C.A. Kuszynski, S.J. Stohs, In Vitr. Mol. Toxicol. 11 (1998) 171–181.
[29] G. Diaz, M.D. Setzu, A. Zucca, R. Isola, A. Diana, R. Murru, V. Sogos, F. Gremo, J. Cell Sci. 112 (1999) 1077–1084.
[30] U.K. Laemmli, Nature 227 (1970) 680–685.
[31] H. Rottenberg, Sh. Wu, Biochim. Biophys. Acta 1404 (1998) 393–404.
[32] P. Privalov, J. Monaselidze, G. Mrevlishvili, V. Magaladze, J. Exp. Theor. Phys. 47 (1964) 2073–2079 (in Russian).
[33] G. Majagaladze, J. Monaselidze, R. Chikvashvili, Differential Microcalorimeter. Author's Certificate N 1267175, USSR (1986).
[34] J.D. Ly, D.R. Grubb, A. Lawen, Apoptosis 8 (2003) 115–128.
[35] N. Touchette, E. Anton, D. Cole, J. Biol. Chem. 261 (1986) 2185–2188.
[36] P. Barboro, A. Pasini, S. Parodi, C. Balbi, B. Cavazza, C. Allera, G. Lazzarini, E. Patrone, Biophys. J. 65 (1993) 1690–1699.
[37] J. Lepock, H. Frey, K. Ritchic, J. Cell Biol. 122 (1993) 1267–1272.
[38] J. Lepock, H. Frey, G. Senisterra, A. Heynen, L. Miriam, Radiat. Res. 2 (1995) 1895–1995.
[39] J. Monaselidze, G. Madjagaladze, N. Bakradze, B. Birkaya, N. Sapojnikova, N. Asatiani, Biophysics 44 (1999) 882–885.
[40] J. Monaselidze, Sh. Barbakadze, Sh. Kvirikashvili, G. Madjagaladze, D. Khachidze, L. Topchishvili, Biomacromolecules 3 (2002) 783–786.
[41] M. Monti, I. Wadso, in: M.N. Jones, (Ed.), Biochemical Thermodynamics, Amsterdam, Oxford, New York, 1979, pp. 257–280.
[42] J. Monaselidze, Z. Chanchalashvili, G. Mgeladze, G. Madjagaladze, J. Polym. Sci. 69 (1981) 17–20.
[43] C. Balbi, M. Adelmoschi, S. Parodi, P. Barboro, B. Cavazza, E. Patrone, Biochemistry 28 (1989) 3220–3229.
[44] M. Bina, J. Sturtevant, A. Stein, Proc. Natl. Acad. Sci. U.S.A. 77 (1980) 4044–4047.
[45] J. Monaselidze, G. Mgeladze, Biofizika 28 (1983) 528–532 (in Russian).
[46] P. Privalov, N. Khechinashvili, J. Mol. Biol. 86 (1974) 665–684.
[47] P. Privalov, Adv. Prot. Chem. 33 (1979) 167–240.
[48] L. Rao, D. Perez, E. White, J. Cell Biol. 135 (1996) 1441–1455.
[49] B. Buenda, A. Santa-Maria, J. Curvalin, J. Cell Sci. 112 (1999) 1743–1753.
[50] D.D. Newmeyer, Sh. Ferguson-Miller, Cell 112 (2003) 481–490.
[51] M. Brand, L. Chien, E. Ainscow, D. Rolfe, R. Porter, Biochim. Biophys. Acta 1187 (1994) 132–139.
[52] M.G. Van der Heiden, N.S. Chandel, E.K. Williamson, P.T. Schumacker, C.B. Thompson, Cell 91 (1997) 627–637.
[53] M.C. Wei, W.X. Zong, E.H. Cheng, T. Lindsten, V. Panoutsakopoulou, A.J. Ross, K.A. Roth, G.R. MacGregor, C.B. Thompson, S.J. Korsmeyer, Science 292 (2001) 727–730.
[54] J.F. Wang, M. Bashir, B.N. Engelsberg, C. Witmer, H. Rozmiarek, P.C. Billings, Carcinogenesis 18 (1997) 371–375.
[55] M.E. Bianchi, M. Beltrame, G. Paonessa, Science 264 (1989) 1134–1137.
[56] C.S. Chow, C. Barnes, S.J. Lippard, Biochemistry 34 (1995) 2956–2964.
[57] C.M. Read, P.D. Cary, C. Crane-Robinson, P.C. Driscoll, M.O.M. Carrillo, D.G. Norman, in: F. Eckstein, D.M.J. Lilley (Eds.), Nucleic Acids and Molecular Biology, Springer Verlag, Berlin, 1995, pp. 222–250.